AD-A094 043 JAYCOR ALEXANDRIA VA F/G 18/1
ECRH STUDIES ON TOKAMAK PLASMAS.(U)
OCT 80 R GILGENBACH N00173-79-C-0472
UNCLASSIFIED JAYCOR-PSD-200-80-009FR NL

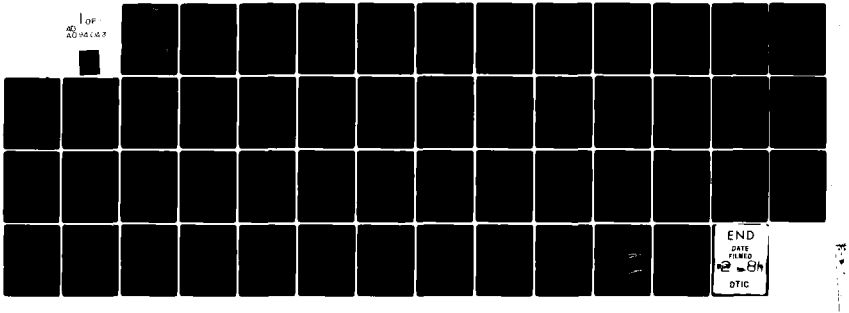

LEVEL II

(2)

AD A094043

JAYCOR

300 Unicorn Park Drive
Woburn, Massachusetts 01801

80 [illegible] 068

ECRH STUDIES ON TOKAMAK PLASMAS

JAYCOR Project No. 6183

Final Report on NRL

Contract No. N00173-79-C-0472

PSD-200-80-009FR

October 10, 1980

Submitted to:

Naval Research Laboratory
Washington, DC

UNCLASSIFIED

SECURITY CLASSIFICATION OF THIS PAGE (When Data Entered)

REPORT DOCUMENTATION PAGE

READ INSTRUCTIONS BEFORE COMPLETING FORM

1. REPORT NUMBER: PSD-200-80-009FR
2. GOVT ACCESSION NO.: AD-A094043
3. RECIPIENT'S CATALOG NUMBER:

4. TITLE (and Subtitle): ECRH STUDIES ON TOKAMAK PLASMAS
5. TYPE OF REPORT & PERIOD COVERED: Final Report 9/17/79 - 9/30/80
6. PERFORMING ORG. REPORT NUMBER: JAYCOR-PSD-200-80-009FR

7. AUTHOR(s): Ronald Gilgenbach
8. CONTRACT OR GRANT NUMBER(s): N00173-79-C-0472

9. PERFORMING ORGANIZATION NAME AND ADDRESS:
JAYCOR
205 South Whiting Street
Alexandria, Virginia 22304

10. PROGRAM ELEMENT, PROJECT, TASK AREA & WORK UNIT NUMBERS:

11. CONTROLLING OFFICE NAME AND ADDRESS:
Naval Research Laboratory
Washington, D.C. 20375

12. REPORT DATE: October 10, 1980
13. NUMBER OF PAGES: 51

14. MONITORING AGENCY NAME & ADDRESS (if different from Controlling Office):

15. SECURITY CLASS. (of this report): Unclassified
15a. DECLASSIFICATION/DOWNGRADING SCHEDULE:

16. DISTRIBUTION STATEMENT (of this Report)
NRL Code 4702
2627
DODAAD Code
S47031

This document has been approved for public release and sale; its distribution is unlimited.

17. DISTRIBUTION STATEMENT (of the abstract entered in Block 20, if different from Report)

18. SUPPLEMENTARY NOTES

19. KEY WORDS (Continue on reverse side if necessary and identify by block number)
ECH
Tokamak
Gyrotron
Plasma Diagnostics
ISX-B
Electron Temperatures

20. ABSTRACT (Continue on reverse side if necessary and identify by block number)
A summary of electron cyclotron heating experiments on the IXS-B Tokamak and the development of electron temperature diagnostics at second harmonic.

DD FORM 1 JAN 73 1473 EDITION OF 1 NOV 65 IS OBSOLETE
S/N 0102-LF-014-6601

UNCLASSIFIED

SECURITY CLASSIFICATION OF THIS PAGE (When Data Entered)

TABLE OF CONTENTS

Section		Page
I.	Introduction	1
II.	Receiver for Detection of Second Harmonic Cyclotron Emission	2
III.	Electron Cyclotron Heating Experiments on the ISX-B Tokamak	3
IV.	Gyrotron Pulse Length Extension	7
	Appendix A. Heating of the Electron Cyclotron Frequency in the ISX-B Tokamak	
	Appendix B. Electron Cyclotron/Upper Hybrid Resonant Preionization in the ISX-B Tokamak	

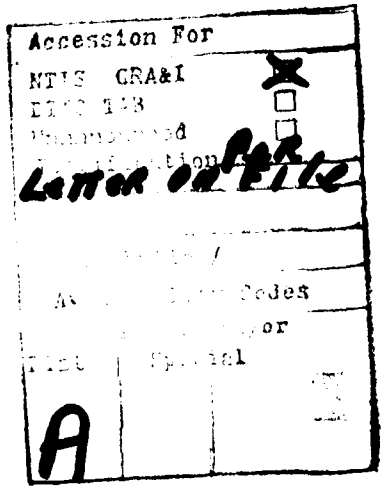

I. INTRODUCTION

In tokamak electron cyclotron heating experiments it is of critical importance to measure the electron temperature at certain points in the plasma. The standard technique for measuring electron temperature has been laser Thomson scattering. However, this diagnostic has the disadvantage that the statistical error bars are relatively large ($\geq$ 10%) especially at low plasma densities. Another diagnostic which has found extensive application in recent years is the measurement of the electron cyclotron emission at the harmonic ($2\omega_c$). If the plasma is sufficiently hot and dense, this emission level is proportional to the electron temperature. The statistical error bars in this case can be as small as 1% of the electron change in temperature. Absolute calibration is still difficult however. This sensitivity to small variations in electron temperature has made this an ideal diagnostic for electron cyclotron heating experiments. This report describes the construction of such a device and its application to the electron cyclotron heating experiments on the ISX-B tokamak. Experimental results are summarized and gyrotron pulse length considerations are discussed.

Appendices A & B are two publications which resulted from this effort. The JAYCOR/NRL/ORNL collaboration was most effective and resulted in a considerable advancement of the current state-of-the-art in ECH knowledge.

II. RECEIVER FOR DETECTION OF THE SECOND HARMONIC CYCLOTRON EMISSION

The detection scheme employed in the ECH experiments was based on the conventional superheterodyne receiver technique. The radiation was collected by an antenna located on the high field side of the tokamak. Theory and experiments have shown that this radiation should be proportional to electron temperature for a sufficiently hot, dense, plasma. The local oscillator frequency was chosen to be 21 GHz. This enabled a measurement of the electron temperature in the region close to the electron cyclotron heated layer. A certain level of nonthermal (signal not proportional to T_e) emission was observed at exactly the second harmonic of gyrotron frequency (20.16 GHz).

It was necessary to operate at relatively low densities in order to avoid a density cutoff of the emitted radiation. Thus most of the experiments were conducted with a line-average electron density of $\sim 10^{13} cm^{-3}$.

III. ELECTRON CYCLOTRON HEATING EXPERIMENTS ON THE ISX-B TOKAMAK

The experimental configuration for the ECH experiments is given in Figure 1. The microwaves (~80 kw) were reflected from a flat plate at the end of an open waveguide. This launching atenna was located almost 180^0 around the tokamak from the second harmonic cyclotron emission diagnostic. The plasma emission at $2\omega_c$ was measured to be black body by varying the tokamak plasma current to obtain a series of different electron temperatures. Comparison with Thomson scattering demonstrated that the second harmonic cyclotron emission level varied linearly with electron temperature.

Experimental results obtained from the cyclotron emission diagnostic are illustrated in Figure 2. The electron temperature measured by Thomson scattering is compared with the cyclotron emission diagnostic in Figure 2b. The agreement between the two diagnositcs is excellent. The dashed curve which indicates the empirical transport code temperature also exhibits a close correspondence between the theory and experiment.

By varying the electron beam current the microwave power level could be increased. The electron temperature shown in Figure 3 varies linearly with microwave power. Again the cyclotron emission data agrees well with Thomson scattering over the full range of electron temperatures. The heating rate of about 6 electron volts per kilowatt is higher than neutral beam electron heating rates, however the 6 ev/kw heating rate has not been normalized to the (decreasing) density.

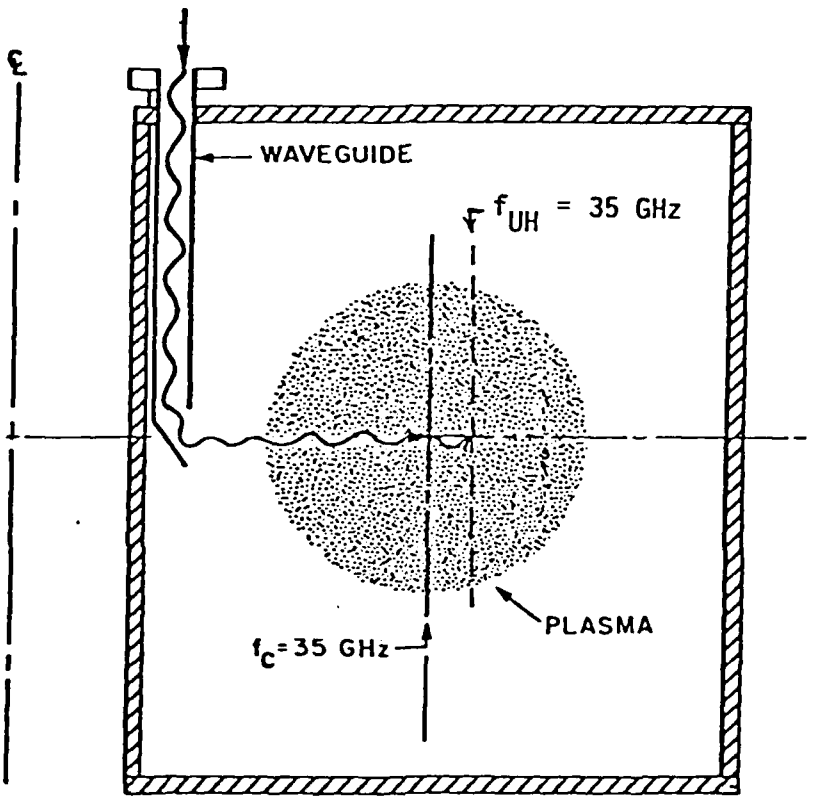

Figure 1. Diagnostic Configuration
for ECH Experiments

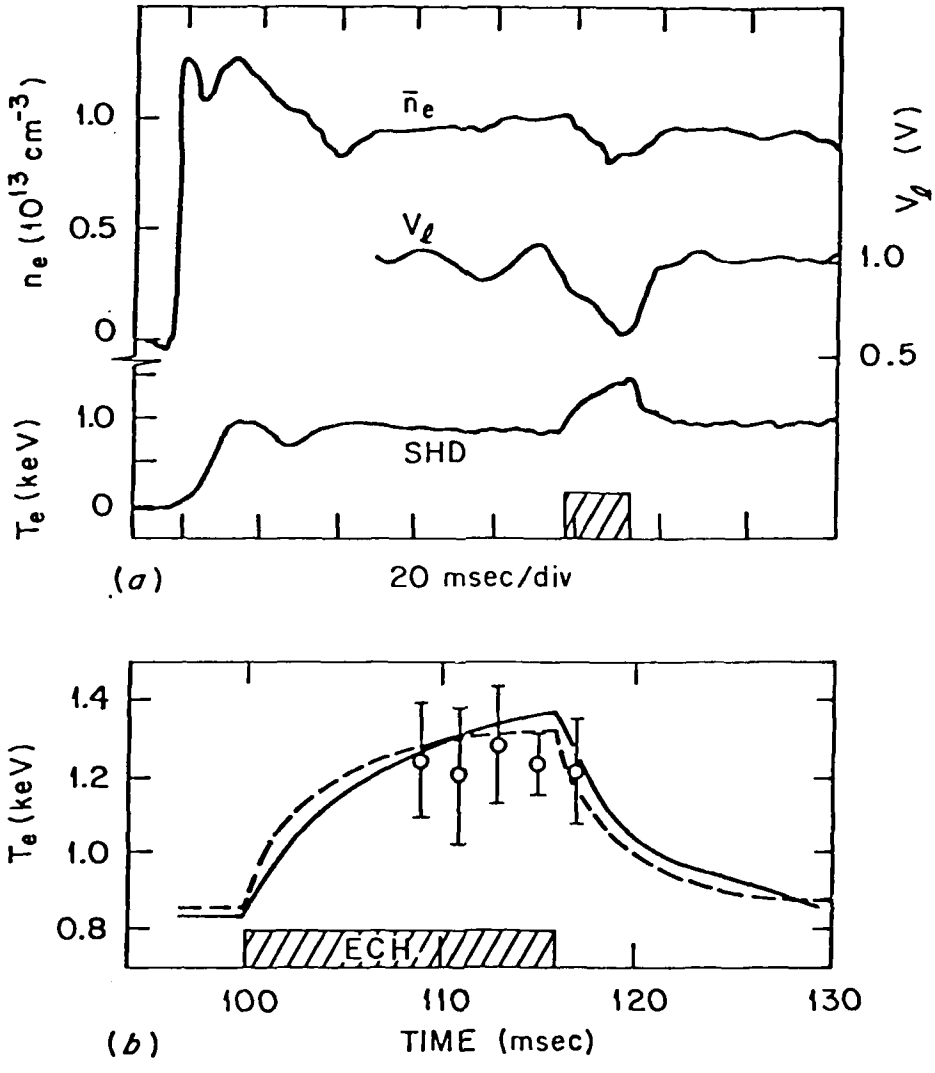

Figure 2. ECH Diagnostics Obtained on ISX-B

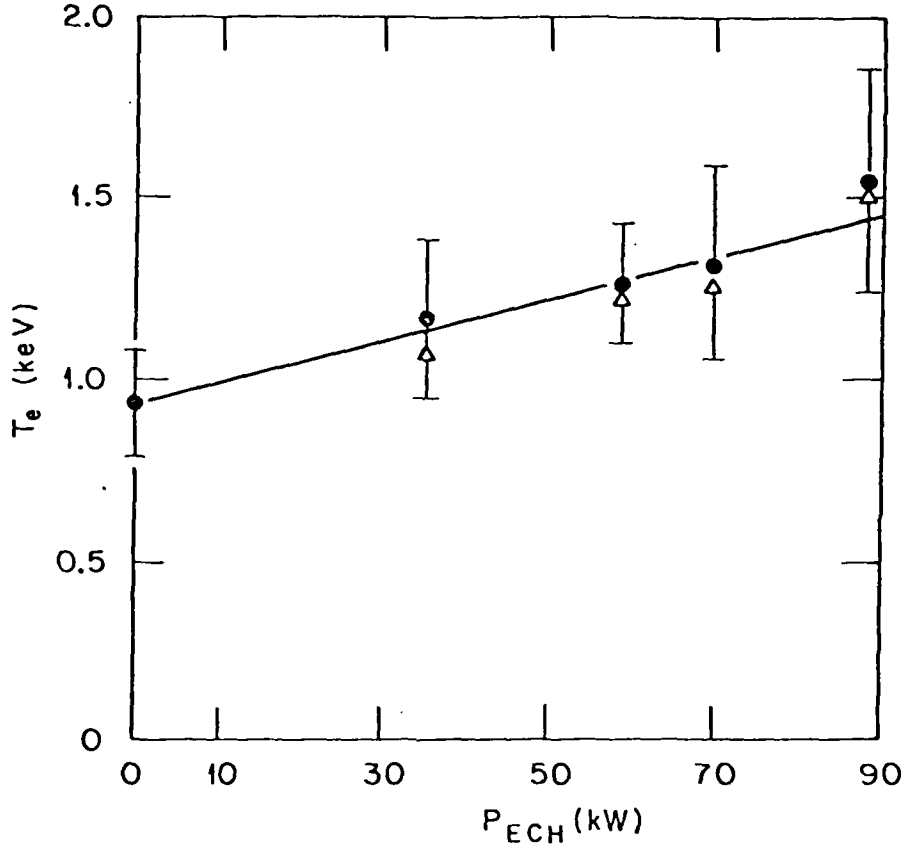

Figure 3. Measured Electron Temperature As A Function Of Microwave Power

IV. GYROTRON PULSE LENGTH EXTENSION

The initial design of the gyrotron collector was for a 10 ms pulse length. Longer pulses were desirable since the energy confinement time of the tokamak was 10 ms. During the course of the ECH experiments it was found that the initial collector design was conservative in that pulses as long as 20 ms were achieved in normal operation. It is now believed that even longer pulses could be produced with the existing collector if an extensive conditioning program were undertaken. Thus, given the above results it was deemed unnecessary to redesign the existing gyrotron collector.

Heating at the Electron Cyclotron Frequency in the ISX-*B* Tokamak

R. M. Gilgenbach,[a] M. E. Read, K. E. Hackett,[b] R. Lucey,[a]
B. Hui, V. L. Granatstein, and K. R. Chu
Naval Research Laboratory, Washington, D. C. 20375

and

A. C. England, C. M. Loring, O. C. Eldridge,[c] H. C. Howe, A. G. Kulchar,[c]
E. Lazarus, M. Murakami, and J. B. Wilgen
Oak Ridge National Laboratory, Oak Ridge, Tennessee 37831
(Received 10 December 1979)

Results are reported of electron-cyclotron-heating experiments in which 80 kW of microwave power from a 35-GHz gyrotron is injected into a tokamak with large single-pass absorption. For 10-ms microwave pulses, incident from the high-field side of the torus, the central electron temperature increases from 850 to 1250 eV, in agreement with empirical transport-code calculations. For the first time it is demonstrated that electron temperature in a tokamak scales linearly with electron-cyclotron-heating power.

Plasma heating by microwaves at the electron cyclotron resonance frequency has been demonstrated to be an effective technique in a variety of confinement devices.[1-3] The recent development of the gyrotron[4] as a high-power, short-wavelength microwave source has made it possible to perform electron-cyclotron-heating (ECH) experiments in tokamaks.[5] Numerous advantages are evident in this method of heating tokamak plasma. As depicted in Fig. 1, the microwave energy can be deposited in a thin resonant layer which exists at the major radius (R) where the electron cyclotron frequency (f_c) is equal to the microwave source frequency (f_g). The microwave absorption coefficient increases with electron temperature[6] T_e, making this an attractive scheme for supplemental heating. The wave damping mechanism is linear and heats the bulk of the electrons, rather than producing a high-energy tail. Antenna structures are small compared with those required for heating at the ion cyclotron or lower hybrid frequencies, since ECH wavelengths are less than 1 cm for most tokamaks.

There exist several theories[7-11] of ECH in tokamaks which predict that the extraordinary wave is more heavily damped than the ordinary wave at oblique incidence from the high-field side. For the parameters of the ISX-*B* (Impurity Study Experiment) tokamak (major radius $R_0 = 93$ cm, minor radius $a = 27$ cm, $T_e = 1$ keV), theory predicts 100% single-pass absorption of the extraordinary wave, while the ordinary wave can undergo about 50% single-pass absorption, depending upon the angle of incidence and the electron density.

Previous experiments by Alikaev *et al.*[5] used short (750 μs) microwave pulses at power levels of less than 60 kW to perform bulk heating in the TM-3 tokamak ($R_0 = 40$ cm, $a = 8$ cm). The energy confinement time, τ_E, in this device was about 300 μs with a plasma current of 60 kA. Because of the small plasma volume and low electron temperature (400 eV) in TM-3, significant single-pass absorption could not occur.[7] Since the unpolarized microwaves were launched from the low-field side of the tokamak, the extraordinary wave component encountered a cutoff and could not propagate directly to the cyclotron resonance.

Here we present the results of ECH experiments in which the larger size of the tokamak and higher electron temperature (~ 1 keV) assure high single-pass microwave absorption. The energy confinement time ($\tau_E = 10$–15 ms) and Ohmic heating power (100–150 kW) in the ISX-*B* are roughly comparable to the Naval Research Laboratory (NRL) gyrotron[12] pulse length (10–20 ms) and output power (100–140 kW). Thus, these experiments provide a significant scaling of the previous ECH research.

The NRL gyrotron oscillator operated at frequency ($f_g = 35.08$ GHz) which corresponds to a resonant field of 12.5 kG with cutoff densities of 1.5×10^{13} cm^{-3} for the ordinary wave and 3×10^{13} cm^{-3} for the extraordinary wave. Microwave output was in the TE_{01} circular mode, which was transmitted to the tokamak with overmoded copper wave guide (6 cm i.d.). Transmission losses between the gyrotron and the tokamak were about 1 dB. As shown in Fig. 1, the microwave power was launched into the plasma from the midplane of the high-field side of the tokamak, eliminating

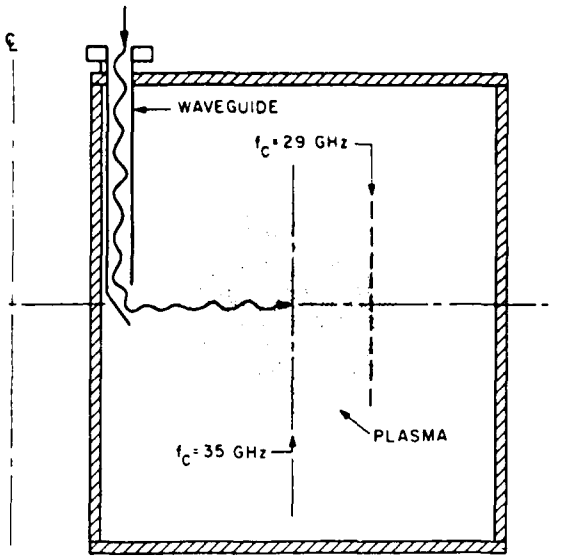

FIG. 1. Experimental configuration. The electron cyclotron frequency (f_c) is shown for a toroidal magnetic field (B_T) of 12.5 kG on axis. The ECH resonant surface (f_c = 35 GHz) is located at the center of the plasma.

the cutoff of the extraordinary wave that occurs on the low-field side. The incident angle was set at 45° from a major radius at the plasma edge. Ray tracing calculations[7] in toroidal geometry predict that this angle of incidence results in almost 100% single-pass absorption of the extraordinary wave and less than 50% single-pass absorption of the ordinary wave. Since the radiated power was an equal mixture of ordinary and extraordinary waves one expects a single-pass heating efficiency of less than 75%. Of the radiation which is not absorbed in a single pass, only a small fraction is reflected directly back to the center of the plasma because of both the extraordinary wave cutoff and the divergence of the microwave beam (± 17°).

Several electron temperature diagnostics were located about 180° around the torus from the antenna. A laser Thomson-scattering system had the capability of four pulses per tokamak shot with pulse separations as small as 1 ms, allowing the time evolution of T_e to be measured during the heating pulse. Detection of the blackbody emission at the second cyclotron harmonic provided a continuous measurement of the electron temperature. This diagnostic utilized a standard superheterodyne receiver, with a local oscillator frequency of 70.5 GHz, and intermediate-frequency amplifier with 60 MHz bandwidth. Detuning the local oscillator from the second harmonic of the gyrotron frequency eliminated the enhanced second-harmonic generation that was observed at exactly $2f_g$. A similar superheterodyne receiver with a local oscillator frequency of 58 GHz measured the electron temperature at a major radius R = 112 cm, as illustrated by the region in Fig. 1 where f_c = 29 GHz.

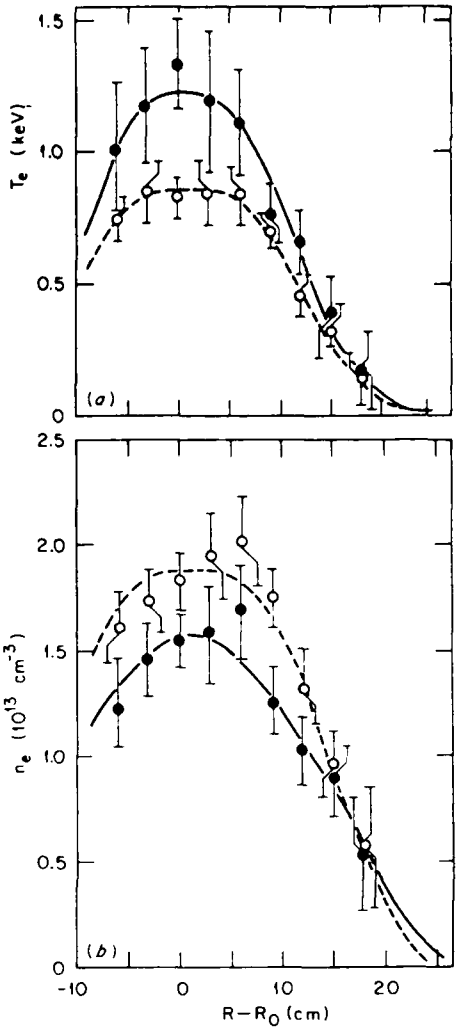

FIG. 2. (a) Electron temperature profile and (b) density profile measured by Thomson scattering. Dashed lines denote data taken before ECH (118 ms into tokamak shot); solid lines represent data at the end of ECH (at 130 ms). Data are for 80-kW microwave injection with a 10-ms ECH pulse starting at 120 ms. B_T was 12.5 kG, line-average electron density ($\bar{n}_e$) was ~10^{13} cm^{-3}, and plasma current (I_p) was 83 kA.

A comparison is given in Figs. 2(a) and 2(b) of the electron temperature and density profiles before and after electron cyclotron resonance heating. These results were obtained with ~ 80 kW of microwave power applied for 10 ms, with the resonant magnetic field located at the center of the plasma. Peak electron density was slightly above the cutoff density for the ordinary wave but below the extraordinary wave cutoff density. The central electron temperature increased from 850 to 1250 eV, becoming more peaked at the center, as expected. This temperature increase is verified by the increase in the second-harmonic cyclotron emission. If one assumes 100% microwave absorption with a Gaussian energy deposition profile centered at the resonant surface, a transport code predicts this temperature increase for an empirical electron heat-conduction coefficient that is independent of T_e. For a microwave input power of 80 kW the heating efficiency is estimated to be about 60% from a power-balance equation that includes (i) the change in plasma electron energy (from 766 to 850 J) divided by the ECH pulse length (10 ms), (ii) the decrease in Ohmic heating power (30 kW), and (iii) the change in electron energy divided by the electron energy confinement time (9.1 ms). During the microwave pulse, the central electron density is seen to decrease by about 15%. This large density decrease was usually observed during the microwave pulse in these experiments. No hard x rays were generated by the ECH, and the soft-x-ray spectrum did not exhibit a high-energy tail, confirming that the bulk of the electrons were heated.

The temporal evolution of the electron density, loop voltage, and central electron temperature are shown in Fig. 3(a) for 80 kW microwave injection with 16 ms ECH pulse duration. Electron temperature at the center of the plasma [Fig. 3(b)] increased from 850 eV to approximately 1300 eV with fairly close agreement between the Thomson-scattering and second-cyclotron-harmonic detection (SHD) diagnostics. An empirical transport code yields a temperature rise and decay that closely resembles the SHD diagnostic. Loop voltage decreased during the ECH pulse from approximately 1.1 to 0.66 V, which, from the Spitzer

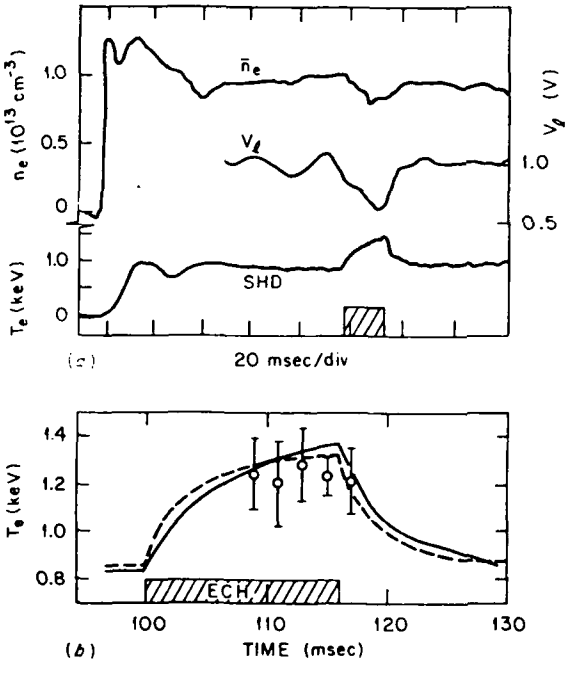

FIG. 3. (a) Central electron temperature (from second-harmonic cyclotron emission), loop voltage (V_l), and line-average electron density vs time for 80-kW microwave pulse of 16-ms duration. (b) Electron temperature measurements from second-cyclotron-harmonic detection are indicated by a solid line, Thomson-scattering measurements by circles, and electron temperature calculated from empirical transport code is shown by dashed line. Plasma parameters were $B_T \cong 12.5$ kG, $\bar{n}_e \cong 10^{13}$ cm^{-3}, and $I_p = 115$ kA.

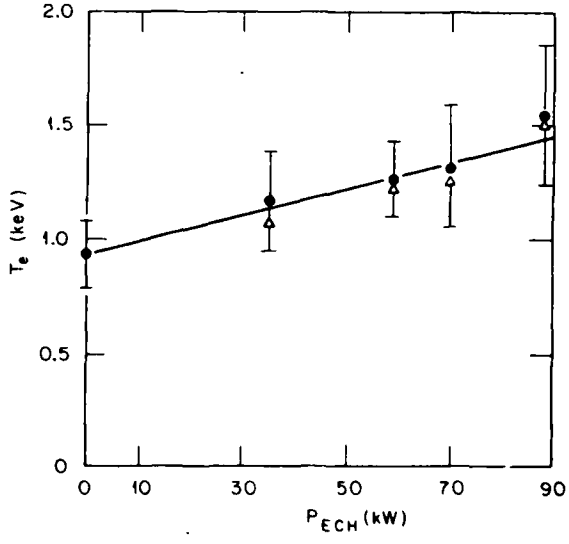

FIG. 4. Central electron temperature vs microwave power with 15-ms ECH pulse length. Electron temperature measured by Thomson scattering (solid circles) and second-harmonic cyclotron emission (triangles). Plasma parameters were $B_T \cong 12.5$ kG, $\bar{n}_e \cong 10^{13}$ cm^{-3}, and $I_p = 85$ kA.

resistivity, indicates an electron temperature increase of about 40%. Both the horizontal and vertical line-average densities decreased by approximately 15% during the heating pulse. A density decrease has also been observed in neutral beam heated plasmas in the ISX-*B*. The experimental density decrease is anomalously large with ECH, since empirical transport-code calculations predict only a 2% decrease in line-average density. This explains why the experimental SHD electron temperatures are slightly higher than the theoretical values in Fig. 3(b).

In order to determine whether the electron cyclotron heating is linear, the gyrotron power was varied. These results, shown in Fig. 4, indicate a linear dependence of T_e on microwave power with a heating rate of ~6 eV/kW. The agreement between the Thomson-scattering data and the second-cyclotron-harmonic detection data is evidence that nonthermal electrons are not produced by ECH. This is the first time that a linear heating rate has been demonstrated for heating at the electron cyclotron frequency in a tokamak.

No ion heating was observed in these ECH experiments. One does not expect ion heating since the low plasma density provides weak coupling between electrons and ions; the microwave pulse lengths (10–16 ms) and energy confinement time (10 ms) are much shorter than the electron-ion equilibration time (~50 ms). However, as tokamaks are scaled toward reactor parameters and gyrotrons with higher frequencies and longer pulses are developed, significant ion heating could occur. Results of the present experiments indicate that ECH may prove to be an important supplementary technique for heating controlled-thermonuclear-reaction plasmas toward ignition temperature.

We gratefully acknowledge the support of J. Sheffield and the entire ISX-*B* tokamak group, especially M. J. Saltmarsh, H. E. Ketterer, S. C. Bates, C. E. Bush, J. L. Dunlap, R. Dyer, R. Isler, T. C. Jernigan, G. H. Neilson, and V. K. Paré. We also thank W. M. Manheimer and E. Ott for useful discussions.

This work was supported by the Office of Fusion Energy, U. S. Department of Energy under the following contracts: No. EX-77-A-34-1015, No. W-7405-ENG-26, and No. ET-78-S-02-4714.

---

[a] Also at JAYCOR, Inc., 205 South Whiting Street, Alexandria, Va. 22304.

[b] Permanent address: Massachusetts Institute of Technology, Cambridge, Mass. 02139.

[c] Also at University of Tennessee, Knoxville, Tenn. 38163.

[1] J. C. Sprott, Phys. Fluids 14, 1795 (1971).

[2] M. Okabayashi, K. Chen, and M. Porkolab, Phys. Rev. Lett. 31, 1113 (1973).

[3] C. L. Hedrick *et al.*, in *Proceedings of the Sixth International Conference on Plasma Physics and Controlled Nuclear Fusion Research, Berchtesgaden, West Germany, 1976* (International Atomic Energy Agency, Vienna, 1977), Vol. 2, p. 145.

[4] V. A. Flyagin *et al.*, IEEE Trans. Microwave Theory Tech. 25, 514 (1977); J. L. Hirschfield and V. L. Granatstein, IEEE Trans. Microwave Theory Tech. 25, 522 (1977).

[5] V. V. Alikaev *et al.*, Fiz. Plasmy 2, 390 (1976) [Sov. J. Plasma Phys. 2, 212 (1976)].

[6] P. C. Efthimion *et al.*, Bull. Am. Phys. Soc. 24, 991 (1979).

[7] E. Ott, B. Hui, and K. R. Chu, to be published.

[8] T. M. Antonsen and W. M. Manheimer, Phys. Fluids 21, 2295 (1978).

[9] O. Eldridge, Phys. Fluids 15, 676 (1972).

[10] I. Fidone *et al.*, Phys. Fluids 21, 645 (1978).

[11] A. G. Litvak *et al.*, Nucl. Fusion 17, 659 (1977).

[12] M. E. Read *et al.*, in *International Electron Devices Meeting* (IEEE Publications, Piscataway, N. J., 1979), p. 172.

ELECTRON CYCLOTRON/UPPER HYBRID RESONANT PREIONIZATION IN THE ISX-B TOKAMAK

R. M. Gilgenbach[a], M. E. Read, K. E. Hackett[b], R. F. Lucey[a], and V. L. Granatstein

Naval Research Laboratory
Washington, D. C.

A. C. England, C. M. Loring, J. B. Wilgen, R. C. Isler, Y-K.M. Peng, K. E. Burrell[c], O. C. Eldridge[d], M. Hacker[c] P. W. King, A. G. Kulchar[d], M. Murakami, R. K. Richards

Oak Ridge National Laboratory
Oak Ridge, Tennessee

ABSTRACT

Preionization experiments have been performed on a tokamak by injecting about 80 kW of microwave power at 35 GHz for up to 15 ms. Microwave absorption occurs at the electron cyclotron and upper hybrid resonance frequencies as predicted by theory. Preionization causes substantial (40%) reductions in loop voltage during the initial phase of the tokamak shot. Flux (volt second) savings with preionization are about 30% in the first 2 ms or about 2% of the total flux expenditure in a tokamak shot. The plasma current begins 200 μs earlier and rises 1.4 times more rapidly in the preionized case. Electron densities of 5×10^{12} cm^{-3} can be sustained throughout the microwave pulse with only a toroidal magnetic field during microwave injection. The bulk electron temperature in the preionized plasma is about 10 eV although there are indications of higher electron temperatures (50 eV) in the upper hybrid resonance layer. Although questions exist concerning the quiescent behavior of the preionized plasma, the observed parameters are shown to be consistent with a theory which employs classical models of energy and particle balance. During the early stages of ohmic heating the preionization is effective in decreasing the peak of the radiated power.

1. INTRODUCTION

Preionization has become an important concept in designing the next generation of large tokamaks. Theory [1] predicts substantial reductions of the loop voltage when a plasma is initiated and heated prior to the onset of toroidal current. The resultant decrease in poloidal field power supply requirements has been shown [1] to have a significant impact on the cost of a large tokamak such as the Engineering Test Facility (ETF). Savings in tokamak poloidal field transformer flux will also permit longer tokamak pulse lengths. Since preionization eliminates the requirement of a large voltage spike for breakdown, it would permit thicker vacuum vessel walls in future tokamaks, enhancing their ability to withstand plasma disruptions. With sufficient power, plasma preheating could cause more rapid "burn-through" the impurity radiation barrier [2].

Typical tokamak start-up techniques now in use or being suggested, include growing the plasma from a small minor radius or applying a negative voltage spike immediately before turning on the forward toroidal voltage. A variety of preionization schemes have been proposed, including injection of neutral beams, relativistic electron beams [3], or microwaves [1]. Plasma heating with microwaves at the electron cyclotron resonant frequency (ω_c) or the upper hybrid resonant frequency (ω_{uH}) has been demonstrated in octupoles [4] and spherators [5] to be an effective technique for heating cold plasma. Recent developments [6] in gyrotron (electron cyclotron maser) technology have provided high power microwave sources at the high frequencies ($\geq$ 28 GHz) required to perform electron cyclotron/upper hybrid resonant preionization and heating in tokamaks. These sources have the advantage that the same equipment may be used for both preionization and bulk heating. [7]

Previous preionization experiments injected short pulses ($\lesssim$ 2 ms) of (10-40 kW) microwaves into a toroidal field device [8], tokapole [9], or tokamak [10]. There is evidence in our experiments on the ISX-B tokamak that longer pulses ($\gtrsim$ 5 ms) are required to examine the "equilibrium" properties of the preionized plasma. In these experiments the injection of (80 kW) unpolarized microwaves for up to 15 ms has enabled us to perform more detailed preionization experiments which can be extrapolated to larger tokamaks.

2. EXPERIMENTAL CONFIGURATION.

The ISX-B (Impurity Studies Experiment) tokamak is an iron core device with a major radius (R_o) of 93 cm and a minor radius (a) of 27 cm. The upper and lower limiter positions allow a plasma elongation ratio of about 2. This tokamak operates in a range of toroidal magnetic fields (10-15 kG) such that the electron cyclotron resonant surface, (at which the source frequency (f_g) is equal to the electron cyclotron frequency [f_c]), can be located at any major radius (R) which is desired. A typical tokamak shot is initiated by discharging a capacitor bank through inner and outer poloidal field windings. This capacitor bank charging voltage was held constant at 400 V in these experiments, thus the 8:1 turns ratio induces a maximum loop voltage of 50 V. The standard gas fill starts 50 ms prior to the toroidal voltage and provides a prefill pressure of about 10^{-4} torr.

The microwave source in these experiments was the NRL 35 GHz gyrotron oscillator [11] which generated 10-16 ms pulses at power levels of 100 kW. Microwave power at $\omega_g/2\pi$ = 35 GHz was transmitted in the TE_{01} mode using (6 cm ID) oversize circular waveguide with about 1 dB attenuation. As depicted in Fig. 1, the microwaves were incident from the midplane of the high field side of the torus with an angle of injection 45^o from a major radius at the plasma edge. The antenna consisted of an open circular waveguide with a reflecting plate which radiated an equal mixture of the ordinary and extraordinary waves. Radiation not absorbed in a single pass could be reflected from the vacuum vessel walls back into the plasma.

A variety of diagnostics were used to measure the electron temperature (T_e) of the preionized plasma in these experiments. A double Langmuir probe was located at the top center of the vacuum chamber, behind the plasma

limiter. The probe ion saturation current was monitored over a series of 18 identical shots with varying probe bias to obtain a characteristic from which the electron temperature could be derived.

An electrostatic particle energy analyzer (PEA) probe was inserted into the plasma to measure the parallel electron temperature and ion saturation current. This probe is similar in design to one used previously in the DIVA tokamak[12]. In this probe the collector current was measured using a logarithmic amplifier, which produced a voltage that varied linearly with selector bias. The selector bias could be swept linearly in time, repetitively during the discharge; if the sweep time is short compared to the time scale over which plasma parameters vary, a set of electron temperatures at multiple discrete times during the discharge is obtained. Alternately, the bias could be held fixed during a discharge and varied from one discharge to the next. This allowed a complete time history of electron temperature at the PEA position to be obtained with a time resolution limited by shot-to-shot reproducibility and by fluctuations in the collected current. The probe could be inserted to various depths in the vacuum vessel or retracted past an isolation valve.

A grazing incidence spectrometer measured the temporal evolution of the oxygen and iron impurity radiation. The electron temperature could be estimated from line radiation data using the RECYCL code [13].

A multiple pulse laser Thomson scattering diagnostic measured the electron temperature and density at as many as 4 discrete times during a tokamak shot. This made it possible to examine the effect of preionization on the temporal evolution of the electron temperature during the current rise phase.

The line-average electron density was measured by two separate 140 GHz microwave interferometers. One of these interferometers measured the average electron density along a vertical chord at the center of the vacuum chamber (R_o = 93 cm), while the other measured the average density along a horizontal chord at the midplane of the tokamak.

A high speed ($\sim$3000 frames/s) movie camera was oriented to view the plasma horizontally, perpendicular to a major radius at the midplane of the tokamak. This permitted observation of the temporal behavior of the plasma in the breakdown stage and ohmic heating stage for both types of discharges, with and without microwave preionization.

3. EXPERIMENTAL RESULTS

Two categories of experiments were performed to determine the properties of the preionized plasma. In the first category, the "toroidal field only" shots, microwave power was injected into the tokamak with the normal gas filling pressure and the toroidal magnetic field (B_T), but no toroidal voltage was applied. The microwave pulses (80 kW) of 15 ms duration ionized the hydrogen in the vessel and produced a low-temperature, poorly-confined plasma with no toroidal current. This plasma was therefore similar to that produced in the second category of "preionization" experiments in which the microwaves were used to preionize the fill gas several milliseconds prior to the initiation of a tokamak discharge.

For the "toroidal field only" shots, the equivalent of a time resolved electron density profile was obtained by measuring the central line-average (l.a.) vertical density ($\bar{n}_{ev}$)and varying the toroidal magnetic field from shot-to-shot. These results, given in Fig. 2, demonstrate that a low density plasma ($\omega_c \simeq \omega_{uH}$), is produced 1 ms after the beginning ($\tau = 0$) of the microwave pulse. The peak density is apparently located at the cyclotron resonance (B_T = 12.5 kG). At τ = 2 ms the peak density apparently moves toward a lower magnetic field, indicating absorption at the upper hybrid resonance. This is confirmed by high speed movies which show that the plasma forms in a narrow resonant layer during the first millisecond and subsequently broadens toward the lower magnetic fields. This behavior is in agreement with theory[1], which predicts that the plasma is initiated in a resonant vertical layer at $\omega_g = \omega_c$ then spreads to a location where $\omega_g = \omega_{uH}$ as the density increases. The interchange instability and $\underline{E} \times \underline{B}$ drift also cause plasma convection toward lower magnetic fields. If one assumes from Fig. 2 that the upper hybrid resonance occurs at a magnetic field of 11.2 kG with a source frequency

($\omega_g = \omega_{uH}$) of 35 GHz, the corresponding density is calculated to be about 3×10^{12} cm^{-3}, in good agreement with the line-average densities of Fig. 2. High speed movies show that after about 5 ms, the plasma attains a configuration determined by the antenna radiation pattern and is confined between the electron cyclotron resonance layer and the outer vacuum vessel wall. This configuration appears to remain quiescent for the last 10 ms of a 15 ms microwave pulse. In these "toroidal field only" experiments, the electron density decays to half its value about 10 ms after the microwaves are turned off. This particle confinement time indicates that the bulk of the plasma electrons are rather cold ($T_e \approx 10$ eV), assuming gradient B drifts.

The line-average horizontal density ($\bar{n}_{eH}$) and vertical density interferometer signals are given in Figures 3(a) and (b) respectively for tokamak shots without and with preionization. Microwaves were injected from t =-7 ms to t = + 2 ms, (where t = 0 corresponds to the onset of the plasma current). For the typical base pressure of 10^{-4} torr the electron density saturated approximately 4 ms after the start of the microwave pulse. With a higher gas filling rate the density increased to 5×10^{12} cm^{-3} throughout a 15 ms microwave pulse. Decreasing the gas filling rate caused the density to saturate more rapidly at the lower value of 2×10^{12} cm^{-3}. This suggests that preionization could permit tokamak startup over a wide range of initial densities without runaway electron generation.

Prior to the application of toroidal current, the plasma is vertically elongated by a factor of 2, corresponding to the poloidal limiter positions. This explains why $\bar{n}_{ev}$ appears greater than $\bar{n}_{eH}$ in Fig. 3(b). After the onset of plasma current, the density increases more gradually in the preionized case, but saturates at the same value after the plasma current reaches its steady state value. Magnetic pickup loops give some indication that the

preionized plasma may be more stable in the first 10 ms of the toroidal current rise.

Typical oscillographs of the loop voltage, electron density, and plasma current are given in Fig. 4 during the first 2 ms of the tokamak shot. The large voltage spike in Fig. 4 (a) is a transient effect since the loop voltage is limited to 50 V by the 8:1 reduction of the 400 V capacitor bank. At 400 μs the loop voltage without preionization is 50 V compared to 30 V when preionizing microwaves were injected from t =-7 ms to + 2 ms. The volt-seconds saved in the first 2 ms amount to 0.01 V-sec or about 30% of the total expenditure during that period. One expects the difference in V_ℓ at 2 ms to be small since the ohmic heating power at this time is large compared to 80 kW of microwave power. With higher microwave power it should be possible to realize savings in loop voltage which persist to later times in the discharge. Preheating by more than 1 ms prior to the application of toroidal voltage produced no further decrease in loop voltage, indicating that the energy confinement time of the hot preionized plasma is short ($\lesssim$ 1ms).

The plasma current was driven by mutual induction from a capacitor bank discharge in poloidal field windings. There was a saturable reactor connected in series with these windings. Although the capacitor bank charging voltage was constant in these experiments, the decay of the capacitor bank current (I_c) was delayed in tokamak shots with preionization. This accounts for the lower loop voltage (V_ℓ) with preionization since the loop voltage is driven by $L\ dI_c/dt$; where L is the mutual inductance between the poloidal field windings and the plasma.

The loop voltage (V_ℓ) consists of the sum of the plasma resistive component ($I_p R_p$) and the inductive component ($L_c\ dI_p/dt$); where I_p is the

plasma current, R_p is the plasma resistance, and L_c is the plasma inductance (internal and external). The inductive component ($L_c dI_p/dt$) of the loop voltage can be estimated by considering the plasma/poloidal field winding system as coaxial conductors with the inductance L_c. The inner conductor (plasma) radius is a = 27 cm, while the outer conductor (poloidal field winding) radius is ρ = 2 a. Plasma/winding inductance is then given by the expression:

$$L_c = \mu_o R_o \left[\ell n(\frac{\rho}{a}) + \frac{1}{4} \right] = 1.1\ \mu H \qquad (1)$$

where μ_o is the free space permeability and ℓn denotes the natural logarithm. Assuming this value of inductance with the plasma current and loop voltage traces given in Fig. 4, one can estimate the inductive and resistive components of the loop voltage. These estimates are summarized in Table I for both the standard discharge and the preionized discharge. It is apparent in Table I that while the inductive loop voltage is approximately equal for the two cases, the resistive loop voltage is much less when preionization is employed. This difference is expected since the microwave injection power (80 kW) heats the electrons directly, causing a significant reduction in the plasma resistivity.

From Fig. 4, it is apparent that the plasma current starts at t = 0 in the preionized case, whereas the current rise is delayed by 200 μs in the standard breakdown. This 200 μs current delay represents transformer flux which is expended in breaking down the fill gas in a standard tokamak discharge. The microwave plasma breakdown thus produces a further volt-second saving from this term. The initial rate of current rise was 1.4 times more rapid when preionization was applied, presumably due to the lower resistive component of the loop voltage.

TABLE I.

SUMMARY OF DATA* WITH ESTIMATES OF INDUCTIVE COMPONENT ($L_c \frac{dI_p}{dt}$) AND RESISTIVE COMPONENT ($I_p R_p$) OF LOOP VOLTAGE (V_ℓ)

	V_ℓ^*(v)	I_p^*(kA)	$L_c \frac{dI_p^*}{dt}$(v)	$I_p R_p$(v)	R_p(mΩ)	$I_p^2 R_p$(kW)
STANDARD DISCHARGE	42	12	15	27	2	288
PREIONIZED DISCHARGE $P_{\mu w}$ = 80 kW from t =-7ms to t = + 2ms	27	20	18	9	0.5	200

*From Fig. 4, at t = 1 ms.

The effect of ECH/UHR preheating on spectral radiation during the early phase of the discharge is illustrated in Fig. 5. The preionization microwave pulse is initiated 7 ms before the ohmic current starts (t = 0) and has a duration of 9 ms. O II and O III are readily produced during this time. The peaks of the radiation from stages O II - O VI are noticeably lower than the levels observed when ohmic heating alone is employed. Similar results are observed in iron, at least through the stage Fe XIV, and the pyroelectric detector which serves as a total radiometer verifies that the power losses immediately following the start-up of the ohmic current are reduced. This reduction of radiative losses clearly leads to conservation of transformer volt-seconds.

The electron temperature resulting from preionization can be estimated from the data of Fig. 5. These estimates are made from the RECYCL Code [13] which is not explicitly time dependent. However, it does allow one to follow the excitation and ionization of particles moving into plasmas with increasing temperature gradients and, hence, is implicitly time dependent. From Fig. 5 it is observed that O II is very near its peak intensity 6 or 7 ms after the preionization pulse is turned on; the line average electron density is 3.8×10^{12} cm^{-3} at this time. Computations indicate that if the confinement time is very long ($\tau >> 10$ ms) this line should reach a maximum when $T_e \approx 10$ eV. However, the oxygen radiation appears to reach a steady state in 5-10 ms and if this period is assumed to represent the confinement time, T_e is calculated to be 11 - 13 eV due to the preionization.

Electron temperature data from the particle energy analyzer (PEA) were obtained at t = 11 msec (after the start of a 15 ms microwave pulse), at three positions. Here the toroidal magnetic field on axis was about 13 kG, thus the ω_c layer was located at R_c = 96 cm and the ω_{uH} layer would be at the major radius R_{uH} = 108 cm. At R = 110 cm (i.e., 2 cm outboard of the ω_{uH} layer) the parallel electron temperature was 45 eV $\pm$ 5 eV. Just inside of the ω_{uH} layer, at R = 106 cm, a temperature of 50 eV $\pm$ 5 eV was measured at t = 11 msec. However, the temperature (at R = 101 cm) between the ω_c layer and the ω_{uH} layer, at t = 14 msec, was found to be only 8.4 $\pm$ 0.8 eV.

The PEA data are consistent with the following picture of the evolution of the plasma during the ECH pulse. At the onset of ECH, the chamber is rapidly (within 1 msec) filled with a uniform, low density, low-temperature plasma, except for a thin layer of hotter, denser plasma localized near the ω_c layer. Later in the ECH pulse, the overall electron density increases, and the high-density, high-temperature layer moves radially outwards, following the upper hybrid resonance layer as the electron density increases. Late in the discharge, then, the PEA will see the low-temperature "background" plasma away from the ω_{uH} layer, but will see higher temperature at larger radii because it is closer to the upper hybrid layer. If the localized layer of hot, dense plasma is sufficiently thin, then spectroscopic temperature measurements, which are line-averaged, will yield a low electron temperature, more characteristic of the background plasma than of the hot layer. This also appears consistent with observations.

Thomson scattering measurements of electron temperature during the current rise phase indicate a higher electron temperature for the preionized discharges. One could explain this in terms of both the lower density (Fig. 3) and the higher current (Fig. 4) early in the shot when preionization was employed.

For the range of gas pressures in these preionization experiments we observed no significant change in the hard X-ray flux from runaway electrons. Both the preionized and standard discharges exhibited hard X-rays only at the end of the tokamak discharge.

It was possible to initiate discharges with lower poloidal field capacitor bank voltage (< 400 V) both with and without preionization. It appeared, however, that when the capacitor bank voltage was lower the ohmic heating power was insufficient to break through the radiation barrier. This resulted in a condition where the entire transformer flux was expended in the burnout phase of the discharge.

4. THEORETICAL ESTIMATES AND INTERPRETATION

The experimental results just presented contain several features that should be discussed more fully. These include: (1) the energy balance for the quasi-steady phase of the discharge, a quiescent plasma with $\bar{n}_e \lesssim 5 \times 10^{12} cm^{-3}$, $T_e \cong 10$ eV and possibly higher ($T_e \cong 50$ eV) near the upper hybrid resonance (UHR); (2) the anomalously fast plasma convection early in the RF pulse, which is probably caused by the interchange instability; (3) the effective absorption of the RF power by the plasma with indications of enhanced absorption at the UHR.

4.1 Particle Balance in the Quasi-Steady Phase.

The plasma parameters are by and large consistent with the assumptions used in Ref. 1, while the particular case considered there assumed 120 kW of extraordinary wave power gave an estimated T_e of about 10 eV throughout the chamber and about 200 eV within a 2 cm thick UHR layer. Assuming that the enhanced absorption at the UHR is limited to the 40 kW in the extraordinary mode, T_e in the present experiment is expected to be significantly less than 200 eV.

If we suspend questions about the stability of the plasma in the absence of toroidal plasma current, an estimate of plasma parameters can be obtained based on relatively straightforward particle and energy balance considerations.

The electron density is determined by a balance between loss through curvature drift and gain from ionization. The curvature drift should dominate in a region free from significant poloidal "stray" field (~ 1 gauss). In ISX-B this region is estimated to be roughly 50 cm by 30 cm around the center of the chamber. We have for nearly steady state:

$$n_e n_o S_H - n_e/\tau_{De} = 0 \qquad (2)$$

where

$$\tau_{De} = 5 \times 10^{-9}\ bRB_T/T_e \ ,$$

S_H is the net ionization rate coefficient, b = 25 cm and cgs units are used except for T_e which is in eV. Equation (2) determines only the neutral density (n_o) as a function of T_e. The values of n_o for T_e = 10 eV and 100 eV are listed in Table II. The theoretical power densities agree quite well with the average experimental power density

$$P_{\mu exp} = 2.7 \times 10^{-2}\ W/cm^3 \ .$$

It is seen that n_o depends only weakly on T_e. So with sufficient electron heating, n_e is determined essentially by the prefill pressure. A density of $n_e \approx 3 \times 10^{12}\ cm^{-3}$ corresponds to a pressure around 10^{-4} torr, which is consistent with the initial amount of gas fill.

4.2 Energy Balance in the Quasi-Steady Phase.

Ions form a channel of energy loss via electron-ion collisional transfer. An estimate of ion temperature (T_i) is needed before assessing the electron energy balance. We have approximately

$$Q_{ie} = \frac{3M_e}{M_i}\frac{n_e(T_e - T_i)}{\tau_{ie}} = \frac{3}{2}\, n_e\left[(T_i - T_e)\, n_o S_{cx} + \frac{T_i}{\tau_{Di}}\right] \ , \qquad (3)$$

where M_e and M_i are respectively the electron and ion mass, τ_{ie} is the electron ion equilibration time, τ_{Di} is the ion diffusion time, and S_{cx} is the charge exchange rate coefficient. Equation (3) assumes that the heating of the ions by collision with the electrons is balanced by charge exchange and curvature drift losses. For $n_e = 3 \times 10^{12}\ cm^{-3}$, Eq. (3) provides an estimate of T_i as

Table II. Estimated Values of Neutral Density, Ion Temperature, and the Required RF Heating Power Density for Several Electron Temperatures with $n_e = 3 \times 10^{12}$ cm^{-3}.

T_e(eV)	10	50	100
$n_o(10^{10}$ cm$^{-3})$	1.1	1.3	2.2
T_i(eV)	9.7	22	14
$P_\mu(10^{-2}$ W·cm$^{-3})$ (ξ = 0)	0.23	2.3	6.4
$P_\mu(10^{-2}$ W·cm$^{-3})$ (ξ = 0.02)	3.8	2.4	6.4

listed in Table II. It is seen that $T_i \approx T_e$ at low $T_e (\sim 10$ eV) while $T_i << T_e$ at high $T_e (\approx 100$ eV). This is apparently due to the large increase of τ_{ie} with increasing T_e.

The energy balance for the electrons can be approximated by,

$$P_\mu = W_{ion}\, n_e n_o S_H + Q_{ie} + \frac{3}{2}\, n_e T_e / \tau_{De} + P_{rad}, \qquad (4)$$

where W_{ion} is the ion energy and the RF heating power (P_μ) is balanced by losses due to ionization, collision with ions, curvature drift and impurity radiation (P_{rad}). Assuming an oxygen content (n_z) of a few percent ($\xi = n_z/n_e \lesssim 0.02$), Eq. (4) shows that P_{rad} dominates when $T_e = 10$ eV, giving an estimate of P_μ as (see Table II)

$$P_\mu \simeq (2.3 \times 10^{-3} + 1.8\xi)\ \mathrm{W/cm^3} \quad . \qquad (5)$$

This shows that the electron energy balance would be dominated by minute amounts of low-Z impurities. For a chamber volume of about 3×10^6 cm^3 and an RF power of 80 kW, Eq. (5) suggests an oxygen content of $\xi \simeq 1.4\%$.

For $T_e \sim 50$ eV to 100 eV, Eq. (4) shows that the electron energy balance would be dominated by loss due to curvature drift and also influenced significantly by ionization and electron-ion collisions if impurity content remains at a few percent. The requirement in P_μ is then estimated to be $2.4 - 6.4 \times 10^{-2}$ W/cm^3. The estimated RF power deposited within a 4-cm layer at the UHR is then 3 kW to 8 kW, respectively. A reduction in ξ by 0.1% in the bulk plasma would provide the surplus RF power to heat the UHR electrons to 50-100 eV.

It is seen that the available data on the RF heated plasma seem consistent with the implications of Eq. (4). Measurements of T_i and n_z are needed to better understand the energy balance during preionization.

4.3 The Interchange Instability.

When a fraction f_μ of microwave power (P_μ = 80 kW) is absorbed in a volume $V_p \approx 3\ m^3$, with an average electron density $\bar{n}_e = 5 \times 10^{12}\ cm^{-3}$, the heating rate of each electron is

$$\frac{d\bar{W}}{dt} = \frac{f_\mu P_\mu}{\bar{n}_e V_p} = f_\mu\ 3.3 \times 10^4\ eV/sec. \qquad (6)$$

The observed electron energy $\bar{W} = 3T_e/2 = 15$ eV gives an energy containment time $\tau_E = 0.45\ msec/f_\mu$. This time can be accounted for by a small concentration of impurities emitting line radiation.

Theoretically, the microwave energy should be deposited in a much smaller volume, producing a higher heating rate and a higher temperature. The impurity radiation would then be much smaller. The interchange instability [14] is probably responsible for the fast convection. The interchange of two tubes of flux that are loaded with plasma is energetically favorable for instability on the outboard side of the tokamak, where the field lines curve away from the plasma. The mechanism for the instability is the short wavelength polarization field produced by the curvature and field gradient drifts [15]. The growth rate is

$$\gamma = V_s[k/R]^{1/2} = [T(eV)/\lambda(cm)]^{1/2}\ 3.3 \times 10^5\ sec^{-1} \qquad (7)$$

where V_s is the sound velocity and $k = 2\pi/\lambda$ is the wave number of the plasma perturbation, which is constant along magnetic field lines. In normal tokamak operation the toroidal current produces a rotational transform that stabilizes this mode. It may also be stable with a sufficiently gentle pressure gradient [1].

4.4 Other Time Scales.

The electron drift from the magnetic field gradient is vertical with a time scale,

$$\tau_M = \frac{M_e \omega_c Rd}{2T_e} = \frac{290 \text{ msec}}{T_e(eV)} \quad , \tag{8}$$

where **d** = 50 cm is the half-height of the chamber. Electrons and ions drift at the same rate in opposite directions. When a charge displacement occurs, a macroscopic electric field develops and both species drift outward together in a time

$$\tau_D = \frac{aB}{Ec} = \frac{110 \text{ msec}}{V(\text{volts})} \quad , \tag{9}$$

where V is the potential and a = 27 cm is the half width.

The motion pictures show that some plasma reaches the top of the machine at the cyclotron resonant surface within a fraction of a millisecond. A few electrons may be heated to kilovolt temperatures very early in the pulse, drifting quickly to the wall.

Ionization by electron impact occurs in a time

$$\tau_i = \frac{1}{n_o S_H} \quad , \tag{10}$$

with a minimum at an electron temperature of $T_e \cong 70$ eV of $\tau_i(\text{min}) = 3.7$ μsec for $n_o = 1 \times 10^{13}$ cm^{-3}. About 35 eV per electron is required for ionization, with most of the energy lost through line radiation. The time τ_i increases as $T_e^{\frac{1}{2}}$ for higher temperature. Electrons travel along field lines around the machine in a time

$$\tau_c = 2\pi R(M_e/T_e)^{\frac{1}{2}} = \frac{13.9 \text{ μsec}}{[T_e(eV)]^{1/2}} \quad , \tag{11}$$

so an electron makes a few toroidal orbits for each ionizing collision.

The electron distribution becomes toroidally isotropic on a time scale

$$\tau_{ee} = 16.3 \text{ nsec } [T_e(\text{eV})]^{3/2} \quad , \tag{12}$$

at the observed density, so it remains isotropic during ionization and heating. As a consequence of these time scales the plasma should be spread uniformly about the torus with no local density maximum near the antenna.

If an electron encounters a field error during each toroidal circuit, one expects the orbit to be displaced and expects a random walk out to the wall. For a step length δ one expects a random walk time

$$\tau_R = \left(\frac{a}{2\delta}\right)^2 \tau_c = \frac{3.2 \text{ msec}}{[\delta(\text{cm})]^2 [T_e(\text{eV})]^{1/2}} \quad . \tag{13}$$

This time and the other containment times do not seem short enough to account for the energy loss. These mechanisms do account for the 10 msec decay time of the afterglow plasma in the experiments with toroidal field only.

4.5 Electron Heating.

Early in the RF pulse one expects linear cyclotron damping to completely absorb the microwave power. For very low electron density the plasma dispersion is negligible and the fraction of microwave power absorbed is

$$f = 1 - \exp(-\eta) \tag{14}$$

where the optical depth is

$$\eta = 2\pi^2 \alpha R/\lambda \quad , \tag{15}$$

with $\alpha = \omega_{pe}^2/\omega_c^2$, ω_{pe} is the electron plasma frequency, θ is the incident angle from the toroidal direction, and where λ is the free space wavelength. The theory is applicable when $\alpha < (2\pi T_e/M_e c^2)^{\frac{1}{2}} \cos\theta$. Total absorption occurs when $n_e > 2 \times 10^{10}$ cm^{-3}. The heating occurs in a small volume of width $\Delta = R \cos\theta \left[T_e/M_e c^2\right]^{\frac{1}{2}}$, determined by the Doppler shift. From either the wave damping or from particle orbits [16] one finds a local heating rate for an average electron

$$\frac{d\bar{W}}{dt} = (2\pi)^{\frac{1}{2}} \frac{e^2}{M_e c^2} \frac{P_\mu}{A} \frac{R\lambda}{\Delta} \exp(-x^2/2\Delta^2) \tag{16}$$

$$= 2.8 \times 10^{10} \exp(-x^2/2\Delta^2) \frac{1}{\Delta(\text{cm})} \text{ eV/sec} \tag{17}$$

where e is the charge of the electron, c is the velocity of light, P = 80 kW, A = 1000 cm^2 is the area irradiated, and x is the distance from the resonant surface. The perpendicular energy gained is rapidly made isotropic and rapidly spread over the entire drift surface. This large heating rate is enough to explain the early vertical drift.

As the density increases the plasma dispersion must be included. One finds [17, 18] an optical depth for the extraordinary wave:

$$\eta \cong \pi^2 \frac{T_e}{M_e c^2} \frac{R}{\lambda} \frac{\cos^2\theta}{\alpha} (2-\alpha)^{3/2}(1+\alpha)^2 \quad , \tag{18}$$

for θ close to 90^0. For the ordinary wave one finds

$$\eta \cong \pi^2 \frac{T_e}{M_e c^2} \frac{R}{\lambda} \alpha(1-\alpha)^{\frac{1}{2}} \quad . \tag{19}$$

For the parameters of this experiment this theory is applicable for $n_e > 1.2 \times 10^{11}$ cm^{-3}. The factor of $T_e/M_e c^2$ appears because both waves are left circularly polarized at cyclotron resonance and absorption depends on the Doppler shift.

The cyclotron absorption of the extraordinary wave is predicted to be complete when $n_e = 1 \times 10^{11}$ cm^{-3}, and to decrease to 9% with $n_e = 5 \times 10^{12}$ cm^{-3} for the temperature observed. Since the waves are launched from the high field side of the tokamak, at the higher density the extraordinary wave propagates to the upper hybrid resonance layer. There it may be absorbed in a nonlinear way or may turn back in the manner first discussed by Stix [19]. The absorption mechanisms are treated in Ref. 1. In any case, the absorption is predicted to be very efficient.

The absorption of the ordinary wave is very small in this density regime. The ordinary mode must be reflected and partially depolarized at the wall before it is absorbed. This multiple pass absorption may still be very efficient since the toroidal chamber has a high quality factor.

The upper hybrid resonance surface at $\omega_g = \omega_{uh} = (\omega_{pe}^2 + \omega_c^2)^{\frac{1}{2}}$ is displaced toward the outer wall of the tokamak. The actual position of the layer depends on the density profile. In the later stages of the discharge the upper hybrid layer may well lie close to the outer wall, and the electron heating zone may be close to the wall, with a small energy containment time.

5. CONCLUSIONS AND DISCUSSION

These experiments have demonstrated that substantial (40%) reductions in loop voltage are obtained in the initial phase of a tokamak discharge when the plasma is preheated by microwaves at the electron cyclotron/upper hybrid resonance frequency. The flux saving from preionization is about 30% of that used in the first 2 ms or 2% of the total volt-seconds expended in a tokamak shot. If these results scale to larger tokamaks (e.g., ETF) they could significantly reduce the poloidal field power supply requirements, also permitting thicker vacuum vessel walls and longer tokamak shots.

Preionization eliminates a 200 μs delay in plasma current rise, thereby saving the transformer flux normally expended in breaking down the prefill gas. The injection of preionizing microwaves causes the plasma current to rise 1.4 times more rapidly than standard discharges. Thus, the plasma could burn through the impurity radiation barrier more rapidly.

Preionized plasma densities of 2-5 x 10^{12} cm^{-3} typically exist with cold electron confinement times of about 10 ms when microwaves are injected with only a toroidal magnetic field. The microwave absorption appears to be at the electron cyclotron frequency for low densities, but as the density increases the absorption apparently occurs at the upper hybrid resonance frequency. The preionized plasma attains a quiescent configuration defined by the antenna radiation pattern between the electron cyclotron resonance and the outer wall. The behavior of the preionized plasma presents an intriguing subject of investigation.

Electron temperatures in the bulk of the plasma have been measured to be 8-13 eV, however, there are indications that electron temperatures in the upper hybrid layer may be as high as 50 eV. The low electron temperatures

(10 eV) agree with other experiments of this type [10], but are lower than the peak temperature predicted theoretically. A possible explanation is that other loss mechanisms are present and that higher temperature electrons are produced only at the upper hybrid resonance region.

ACKNOWLEDGEMENTS

We gratefully acknowledge the support of J. Sheffield and the entire ISX-B tokamak group, especially M. J. Saltmarsh, H. E. Ketterer, S. C. Bates, C. E. Bush, J. L. Dunlap, R. Dyer, T. C. Jernigan, J. L. Lyon, G. H. Neilson, V. K. Paré, and D. W. Swain. We also thank S. K. Borowski, and W. M. Mannheimer for useful discussions.

This work was supported by the Office of Fusion Energy, U.S. Department of Energy under the following contracts: (i) Contract No. EX-77-A-34-1015 with the Naval Research Laboratory; (ii) Contract No. W-7405-ENG-26 with the Union Carbide Corporation; (iii) Contract No. ET-78-S-02-4714 with the Massachusetts Institute of Technology.

(a) JAYCOR, Alexandria, Virginia 22304.

(b) MIT, Cambridge, Massachusetts 02139.

(c) General Atomic Corporation, La Jolla, California.

(d) University of Tennessee, Knoxville, Tennessee 38163.

REFERENCES

1. Peng, Y-K.M., Borowski, S. K., and Kammish, T., Nucl. Fusion 18 (1978) 1489.

2. Hawryluk, R. J., and Schmidt, J. A., Nucl. Fusion 16 (1976) 775.

3. Mohri, A., Narihara, K., Tsuzuki, T., Kubota, Y., Tomita, Y., et al, in Plasma Physics and Controlled Nuclear Fusion Research (Proc. 7th Int. Conf., Innsbruck) IAEA-CN-37-X-5, Aug. 1978.

4. Sprott, J. C., Phys. Fluids 14 (1971) 1795.

5. Okabayashi, M., Chen, K., Porkolab, M., Phys. Rev. Lett. 31 (1973) 1113.

6. Flyagin, V. A., Gapunov, A. V., Petelin, M. I., and Yulpatov, V. K., IEEE Trans. Microwave Theory Tech. 25 (1977) 514; Hirschfield, J. L. and Granatstein, V. L., IEEE Trans. Microwave Theory Tech. 25 (1977) 522.

7. Gilgenbach, R. M., Read, M. E., Hackett, K. E., Lucey, R. F., Hui, B., et al, Phys. Rev. Lett. 44 (1980) 647.

8. Anisomov, A. I., Vinogradov, N. I., Poloskin, B. P., Sov. Phys. Tech. Phys. 18 (1973) 459; 20 (1976) 626; 20 (1976) 629.

9. Holly, D. F., Witherspoon, D. F., Sprott, J. C., Bull. Am. Phys. Soc. 23 (1978) 878.

10. Bulyginsky, D. G., Larionov, M. M., Levin, L. S., Miklukho, O. V., Tokunov, A. I., et al, Ioffe Physical Institute Report #611 (1979).

11. Read, M. E., Gilgenbach, R. M., Lucey, R. F., Chu, K. R., and Granatstein, V. L., "Spatial and Temporal Coherence of a 35 GHz Gyromonotron Using the TE_{01} Circular Mode" IEEE Trans. on Microwave Theory Tech. (to be published).

12. Kimura, H., Nuclear Fusion 18 (1978) 1195.

13. Isler, R. C., Crume, E. C., and Howe, H. C., Nucl. Fusion 19 (1979) 727.

14. Callen, J. D., private communication.

15. Rosenbluth, M. N., and Longmire, C. L., Ann. Phys. 1 (1957) 120.

16. Eldridge, O. C., Phys. Fluids 15 (1972) 676.

17. Litvak, A. G., Permitin, G. V., Surorov, E. V., Frajman, A. A., Nucl. Fusion 17 (1977) 654.

18. Eldridge, O. C., Namkung, W., England, A. C., ORNL Technical Memorandum TM-6052, Oak Ridge National Laboratory (Nov. 1977).

19. Stix, T. H., Phys. Rev. Lett. 15 (1965) 878.

FIGURE CAPTIONS

Fig. 1 - Experimental configuration. Unpolarized microwaves are launched from a reflecting plate antenna located on the high field side of the torus. The location of the electron cyclotron resonant surface (f_c = 35 GHz) and upper hybrid resonant surface (f_{uH} = 35 GHz) are shown for a toroidal magnetic field on axis B_T = 12.5 kG and an electron density of 3 x 10^{12} cm^{-3}.

Fig. 2 - Line-average electron density measured through a vertical chord at the center of the vacuum vessel. By varying the toroidal magnetic field from shot-to-shot the equivalent of a time resolved density profile was obtained.

Fig. 3 - Temporal evolution of the line-average electron density measured vertically ($\bar{n}_{eV}$) and horizontally ($\bar{n}_{eH}$) for conditions:
(a) standard tokamak discharge without preionization, and
(b) tokamak discharge with preionizing microwaves injected from t = - 7 ms to t = + 2 ms.

Fig. 4 - Temporal evolution of the loop voltage (V_ℓ), horizontal line-average electron density (n_e), and plasma current (I_p) for conditions:
(a) standard tokamak discharge without preionization and,
(b) tokamak discharge with 80 kW preionizing microwaves injected from t = - 7 ms to t = + 2 ms.

Fig. 5 - Spectral radiation measured by grazing incidence spectrometer. The solid lines denote data taken during standard tokamak discharge without preionization. Dashed lines denote data taken

during tokamak discharge with 80 kW microwaves injected at times indicated by crosshatched areas.

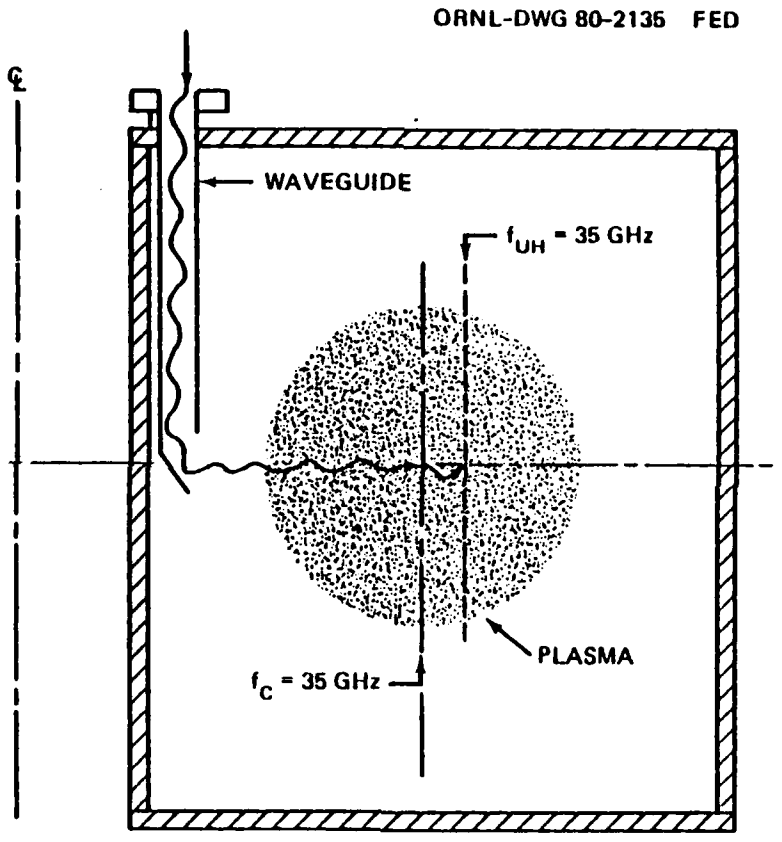

Figure 1

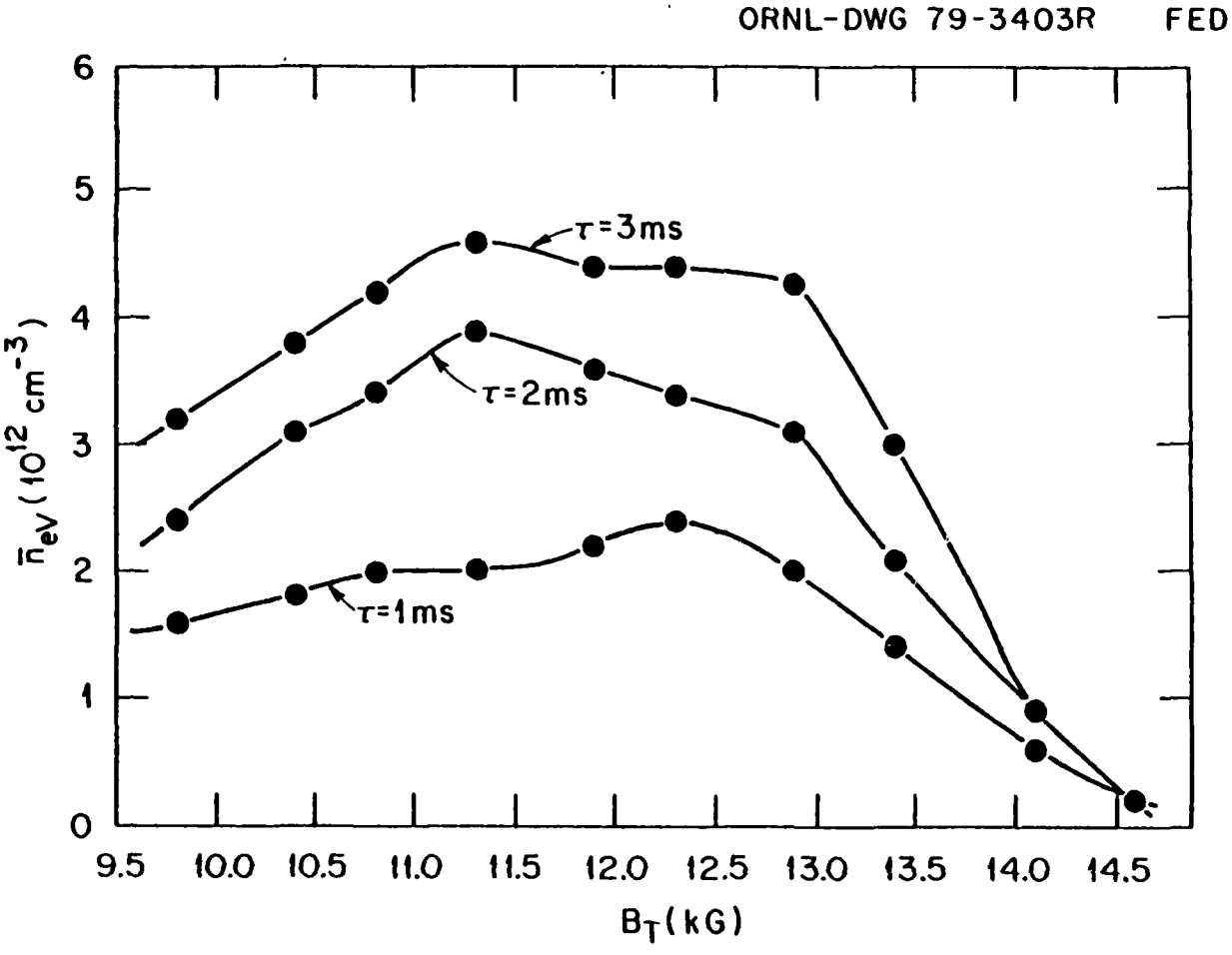
ORNL-DWG 79-3403R FED
6
5
4
3
2
1
0
$\bar{n}_{eV}$ (10^{12} cm^{-3})
τ=3ms
τ=2ms
τ=1ms
9.5
10.0
10.5
11.0
11.5
12.0
12.5
13.0
13.5
14.0
14.5
B_T (kG)

Figure 2

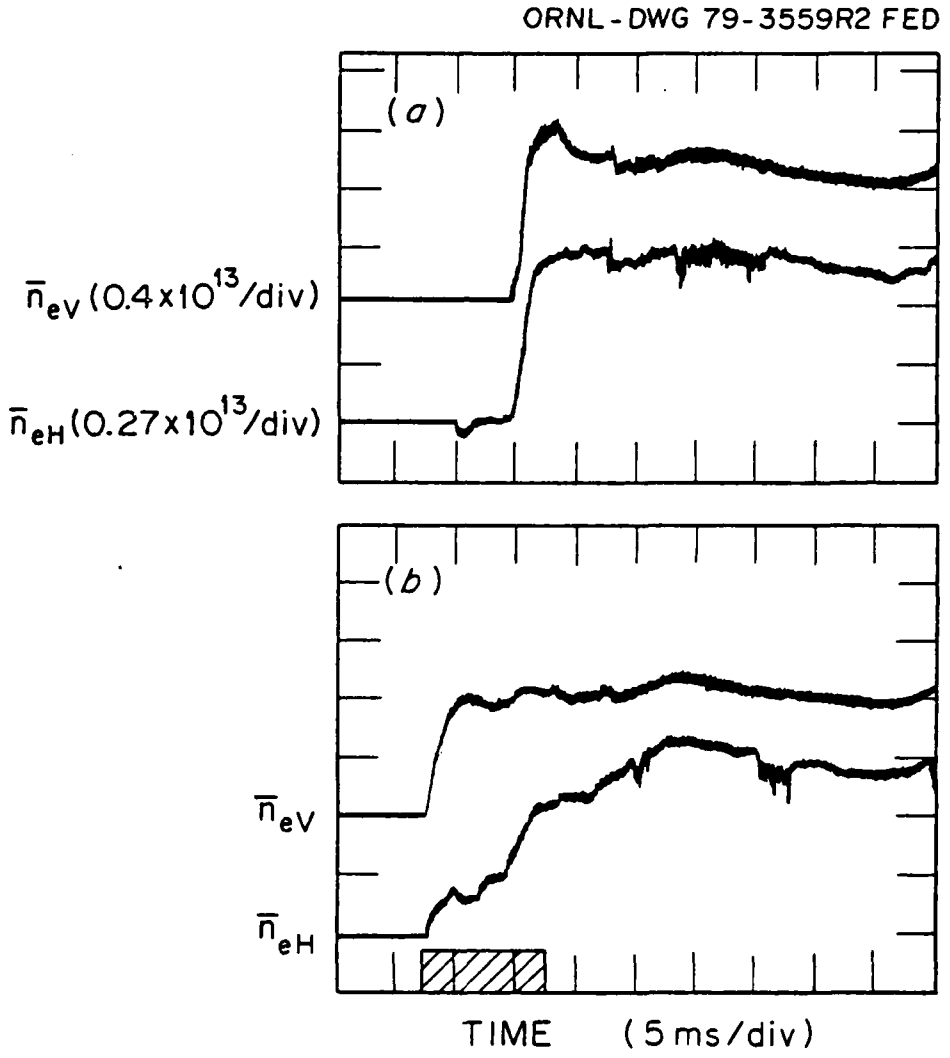
ORNL-DWG 79-3559R2 FED
(a)
$\bar{n}_{eV}$ (0.4x10^{13}/div)
$\bar{n}_{eH}$ (0.27x10^{13}/div)
(b)
$\bar{n}_{eV}$
$\bar{n}_{eH}$
TIME (5 ms/div)

Figure 3

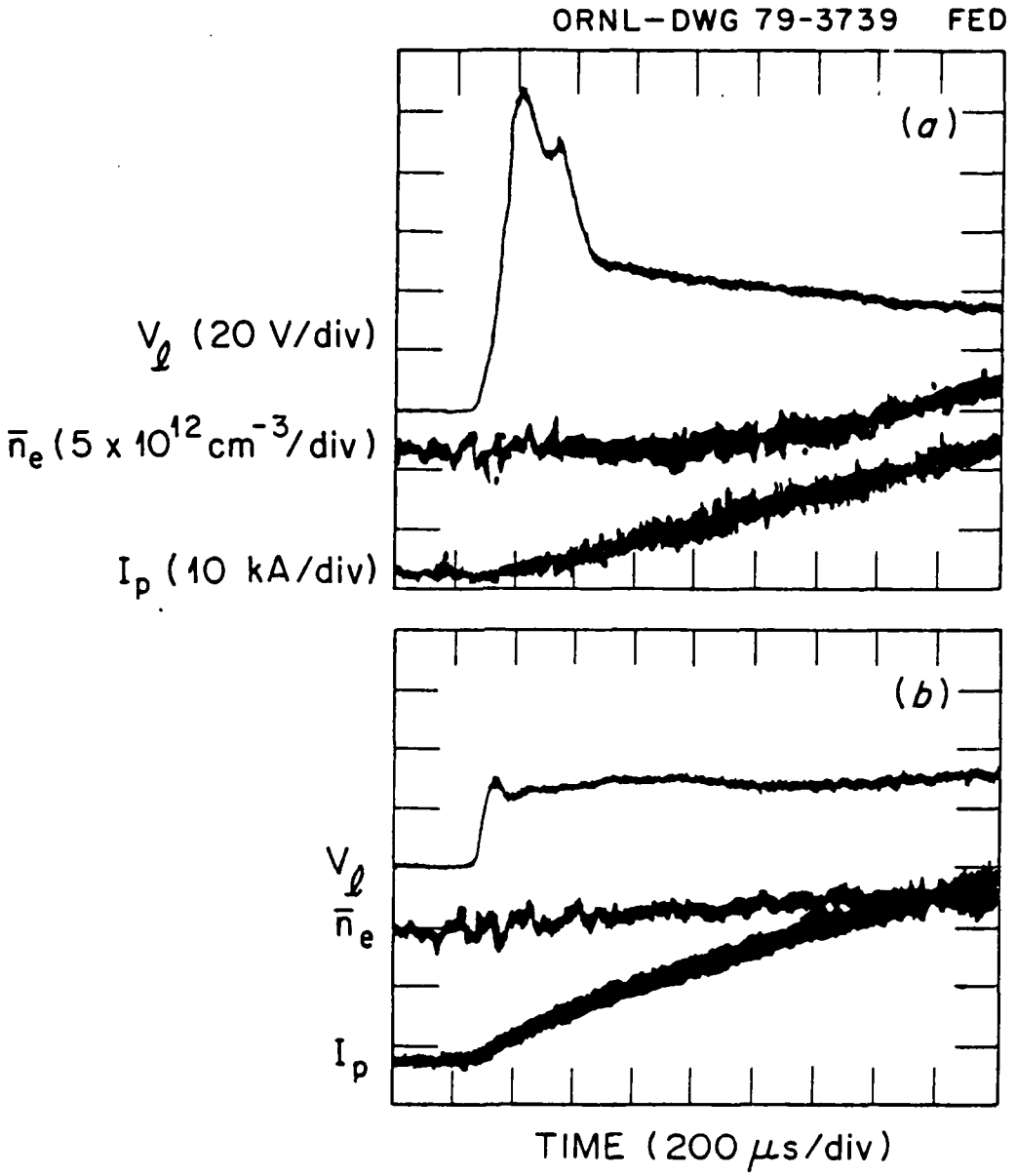
ORNL-DWG 79-3739 FED
(a)
V_ℓ (20 V/div)
$\bar{n}_e$ (5×10^{12} cm^{-3}/div)
I_p (10 kA/div)
(b)
V_ℓ
$\bar{n}_e$
I_p
TIME (200 μs/div)

Figure 4

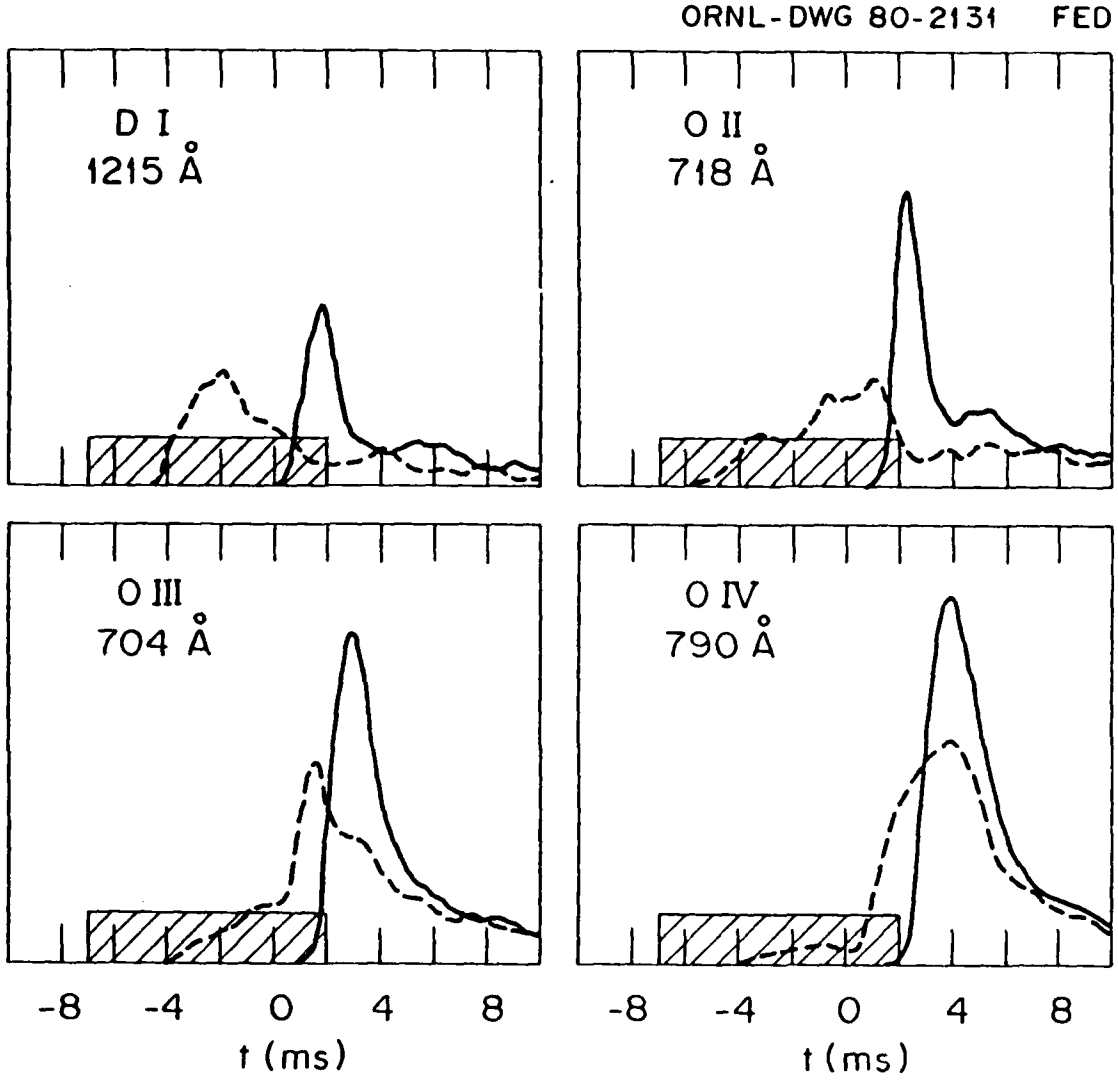
ORNL-DWG 80-2131 FED
D I
1215 Å
O II
718 Å
O III
704 Å
O IV
790 Å
-8
-4
0
4
8
t (ms)
-8
-4
0
4
8
t (ms)

Figure 5

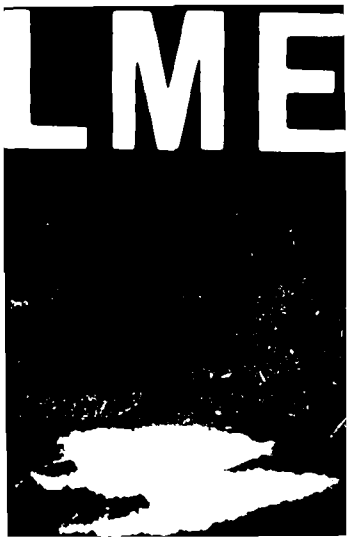
LME